Inorganic Chemistry

Article

pubs.acs.org/IC

Mononuclear and Tetranuclear Compounds of Yttrium and Dysprosium Ligated by a Salicylic Schiff-Base Derivative: Synthesis, Photoluminescence, and Magnetism

Munendra Yadav,[†] Valeriu Mereacre,[†] Sergei Lebedkin,[‡] Manfred M. Kappes,*[,‡,§] Annie K. Powell,*[,†,‡] and Peter W. Roesky*[,†]

[†]Institut für Anorganische Chemie, Karlsruher Institut für Technologie, Engesserstrasse 15, 76131 Karlsruhe, Germany

[‡]Institut für Nanotechnologie, Karlsruher Institut für Technologie, Postfach 3640, 76021 Karlsruhe, Germany

[§]Institut für Physikalische Chemie, Karlsruher Institut für Technologie, Fritz-Haber Weg 2, 76131 Karlsruhe, Germany

Supporting Information

ABSTRACT: The Schiff-base (2-aminoethyl)hydroxybenzoic acid (H_2L) as a proligand was prepared in situ from 3-formylsalicylic acid and ethanolamine (ETA). The mononuclear {[Y(HL)$_4$][ETAH]·H_2O} (**1**) and {[Dy(HL)$_4$][ETAH]·3MeOH·H_2O} (**2**) and tetranuclear {[Y_4(HL)$_2$(L)$_4$(μ_3-OH)$_2$]·4MeOH·4H_2O} (**3**), {[Dy_4(HL)$_2$(L)$_4$(μ_3-OH)$_2$]·5(MeOH)$_2$·7H_2O (**4**), and {[Dy_4(HL)$_8$(L)$_2$]·4MeOH·2H_2O}(**5**) rare-earth metal complexes of this ligand could be obtained as single-crystalline materials by the treatment of H_2L in the presence of the metal salts [Ln(NO$_3$)$_3$·(H$_2$O)$_m$] (Ln = Y, Dy). In the solid state, the tetranuclear compounds **3** and **4** exhibit butterfly structures, whereas **5** adopts a rectangular arrangement. Electrospray ionization mass spectrometry data of the ionic compounds **1** and **2** support single-crystal X-ray analysis. The yttrium compounds **1** and **3** show fluorescence with 11.5% and 13% quantum yield, respectively, whereas the quantum yield of the dysprosium complex **4** is low. Magnetic studies on the dysprosium compounds **4** and **5** suggest the presence of weak antiferromagnetic interactions between neighboring metal centers. Compound **4** shows single-molecule-magnet behavior with two relaxation processes, one with the effective energy barrier U_{eff} = 84 K and the preexponential factor $\tau_0 = 5.1 \times 10^{-9}$ s.

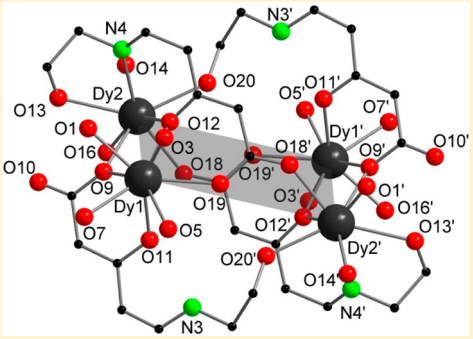

INTRODUCTION

Since the discovery of single-molecule-magnet (SMM) behavior, research efforts have focused on the design of compounds with high blocking temperatures and high energy barriers to spin reversal with the prospect of developing systems with applications in high-density data storage, molecular spintronics, and quantum computing devices.[1−6] The general approach to creating new SMMs is to aim for systems with enhanced negative Ising (or easy-axis) types of magnetoanisotropy (D) and large ground spin states.[7−11] Recently, interest in molecular magnets incorporating lanthanide ions has been revived, and 4f coordination compounds have been extensively investigated for their SMM and single-ion-magnet (SIM) properties.[9,12−20] In particular, ions with high spins and intrinsic magnetic anisotropy along with strong orbital coupling such as dysprosium(III), terbium(III), and holmium(III) have proven to be of interest.[21] While the (Bu_4N)[Tb(Pc)$_2$] (H_2Pc = phthalocyanine) molecule was the first example of a pure 4f compound showing SMM behavior (and because it involves a single ion, this is also described as SIM behavior), it has generally been found that compounds involving the highly anisotropic dysprosium(III) ion provide systems with the best SMM properties.[22−44] This partly arises from the fact that the terbium(III) ions are much more sensitive to distortions from idealized coordination geometries in terms of optimized single-ion anisotropy.[13,16−22]

Recent work from our group has involved Schiff-base ligands derived from 4-formyl-3-hydroxybenzoic acid for use in the coordination chemistry of the rare-earth elements. For example, by using *N*,*N*′-bis(4-carboxysalicylidene)ethylenediamine as the ligand, a mixed nickel/dysprosium complex showing slow relaxation of magnetization below 12 K was reported.[45] In addition, the multidentate proligand 2,2′-{[(2-aminoethyl)-imino]bis[2,1-ethanediylnitriloethylidyne]}bis(2-hydroxybenzoic acid) (H_4L') was synthesized and gave the mononuclear dysprosium(III) complex [Dy(H_3L)$_2$](NO$_3$)·EtOH·8H_2O showing SIM behavior.[46]

Herein we report the synthesis and application of the multidentate Schiff-base proligand (2-aminoethyl)-hydroxybenzoic acid (H_2L) in the coordination chemistry of rare-earth elements (Scheme 1). H_2L, which was described before,[47] was prepared in situ from 3-formylsalicylic acid and

Special Issue: To Honor the Memory of Prof. John D. Corbett

Received: June 25, 2014
Published: September 19, 2014

ethanolamine. Magnetic and photophysical properties of the new compounds were determined.

Scheme 1. Synthesis of H_2L

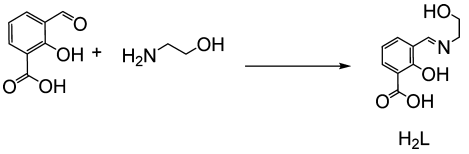

H_2L

EXPERIMENTAL SECTION

General Considerations. IR spectra were obtained on a Bruker FTIR Tensor 37 via the attenuated total reflection (ATR) method. Elemental analyses were carried out with an Elementar Vario EL or Vario Micro Cube. Electrospray ionization mass spectrometry (ESI-MS) was performed in positive and negative ionization modes using an IonSpec FT-ICR (7T). (2-Aminoethyl)hydroxybenzoic acid (H_2L) was prepared according to literature procedures.[47] The other chemicals were purchased from commercial sources and used without further purification.

Photoluminescence (PL) Measurements. PL measurements were performed on a Horiba JobinYvon Fluorolog-322 spectrometer equipped with a closed-cycle optical cryostat (Leybold) operating at ∼20−300 K. Hamamatsu R9910 and R5509 photomultipliers were used as detectors in the emission spectral ranges of ∼300−850 and ∼600−1400 nm, respectively. Solid samples (crystalline powders) were dispersed in a thin layer of polyfluoroester oil (ABCR GmbH) between two 1 mm quartz plates. These were mounted on the coldfinger of the cryostat. The emission spectra were corrected for the wavelength-dependent response of the spectrometer and detector (in relative photon flux units).

For PL quantum yield (PLQY) measurements (at an ambient temperature of 295 K), a 10 cm integrating sphere made of optical poly(tetrafluoroethylene) with low autoluminescence (Berghof GmbH) was installed in the sample chamber of the spectrometer. Samples were inserted into the sphere in 1 mm glass tubes and excited at 420 nm. The emission spectra, relative absorption at the excitation wavelength, and, correspondingly, PLQYs were referenced to those of a Coumarin 307 laser dye dissolved in methanol, according to a previously described procedure.[48] The PLQY of Coumarin 307 was taken as 0.95.[48] The accuracy of the determination of PLQY was estimated to be ±10%.

Magnetic Measurements. The magnetic measurements were carried out using a Quantum Design SQUID magnetometer MPMS. This magnetometer works between 1.8 and 400 K for direct-current (dc) applied fields ranging from −70 to +70 kOe. Measurements were performed on polycrystalline samples dispersed in Apiezon grease.

Synthesis of (2-Aminoethyl)hydroxybenzoic acid (H_2L).[47] A solution of 3-formylsalicylic acid (0.4 mmol) and ethanolamine (ETA; 0.4 mmol) was stirred at room temperature in 5 mL of ethanol for 2 h. The resulting yellow solid was filtered and dried in a vacuum.

Yield: 60 mg (71.7%). Anal. Calcd for $C_{10}H_{11}NO_4$: C, 57.41; H, 5.30; N, 6.70%. Found: C, 57.19; H, 5.30; N, 6.66%. IR (ATR): ν 3215 (br), 1652 (s), 1552 (m), 1469 (m), 1329 (w), 1250 (w), 1220 (w), 1154 (w), 1057 (m), 1022 (s), 903 (w), 886 (w), 759 (s), 710 (w), 614 (w), 549 (w) cm^{-1}. ^1H NMR (300 MHz, DMSO-d_6): δ 12.89 (br, 2 H), 8.72 (s, 1 H), 8.08 (d, J = 7.3 Hz, 1 H), 7.69 (d, J = 7.0 Hz, 1 H), 6.68 (t, J = 7.6 Hz, 1 H), 5.18 (t, J = 4.5 Hz, 1 H), 3.76 (d, J = 3.6 Hz, 2 H), 3.70 (m, 2 H). $^{13}C\{^1H\}$ NMR (75 MHz): δ 175.2 (carboxyl), 169.1, 168.3, 141.1, 139.9, 119.5, 116.1, 114.1 (aromatic), 59.3, 54.1 (alkyl chain).

*Synthesis of {[Ln(HL)$_4$][ETAH]} (**1** and **2**).* $Ln(NO_3)_3{\cdot}6H_2O$ (Ln = Y, Dy; 0.1 mmol) was treated with the Schiff-base H_2L, which was formed in situ by condensation of an excess of ETA (1.5 mmol) and 3-formylsalicylic acid (0.4 mmol) in 10 mL of methanol and in the presence of pyridine (0.6 mmol). The slight excess of ETA is essential for formation of the complex. The resulting yellow solution was stirred for 20 min at room temperature and subsequently filtered. The filtrate was left undisturbed to allow slow evaporation of the solvent. Yellow single crystals suitable for X-ray diffraction analysis formed within 1 week.

*{[Y(HL)$_4$][ETAH]·H$_2$O} (**1**).* Yield: 30 mg (single crystals; 30% based on the metal salt). Anal. Calcd for $C_{42}H_{50}YN_5O_{18}$: C, 50.36; H, 5.03; N, 6.99%. Found: C, 49.53; H, 5.01; N, 6.95%. ESI-MS: 921.17 ($[Y(HL)_4]^-$). IR (ATR): 3088 (w, $\upsilon_{C=C-H}$), 1652 (m), 1603 (m), 1540 (s), 1482 (w), 1455 (w), 1380 (m), 1306 (w), 1213 (m), 1149 (w), 1070 (w), 1050 (s), 1023 (w), 953 (w), 920 (w), 874 (s), 835 (w), 791 (w), 769 (m), 696 (w), 646 (m), 622 (w), 577 (w), 538 (w), 510 (w) cm^{-1}.

*{[Dy(HL)$_4$][ETAH]·3MeOH·H$_2$O} (**2**; ETAH = Protonated ETA = Ethanolammonium).* Yield: 40 mg (single crystals; 34% based on the metal salt). Anal. Calcd for $C_{45}H_{60}DyN_5O_{20}$ (corresponds to **1**·H_2O): C, 46.86; H, 5.24; N, 6.07%. Found: C, 45.60; H, 4.74; N, 6.47%. ESI-MS: 995.0 ($[Dy(HL)_4]^-$). IR (ATR): ν 3069 (w, $\upsilon_{C=C-H}$), 2947 (w, υ_{C-H}), 2849 (w), 1652 (m), 1604 (m), 1539 (s), 1480 (w), 1449 (w), 1377 (m), 1304 (w), 1272 (w), 1235 (w), 1212 (m), 1149 (w), 1070 (w), 1050 (s), 1023 (w), 953 (w), 920 (w), 874 (s), 835 (w), 791 (w), 770 (m), 696 (w), 646 (m), 622 (w), 577 (w), 538 (w), 510 (w) cm^{-1}.

*Synthesis of {[Y$_4$(HL)$_2$(L)$_4$(μ_3-OH)$_2$]·4MeOH·4H$_2$O} (**3**).* $[Y(NO_3)_3{\cdot}6H_2O]$ (0.19 mmol) was treated with the Schiff-base H_2L, which was formed by in situ condensation of ETA (0.4 mmol) and 3-formylsalicylic acid (0.4 mmol) in 10 mL of methanol. The resulting yellow solution was stirred for 3 h at room temperature; at the end of stirring, Et_3N (0.1 mmol) was added, and the solution was filtered. The filtrate was left undisturbed to allow slow evaporation of the solvent. Yellow single crystals of **3** suitable for X-ray diffraction analysis formed after 1 week. Yield: 20 mg (single crystals; 6% based on the metal salt). Anal. Calcd for $C_{64}H_{82}N_6O_{34}Y_4$: C, 41.89; H, 4.50; N, 4.58%. Found: C, 40.02 H, 4.10; N, 5.45%. IR (ATR): ν 3062 (br, $\upsilon_{C=C-H}$), 1653 (w), 1641 (m), 1606 (s), 1555 (s), 1506 (w), 1476 (w), 1457 (m), 1432 (m), 1362 (s), 1304 (w), 1274 (w), 1217 (w), 1150 (m), 1112 (w), 1077 (w), 1048 (m), 967 (w), 915 (w), 872 (m), 830 (w), 803 (w), 755 (m), 660 (w), 645 (s), 629 (w), 572 (w), 536 (w) cm^{-1}.

*Synthesis of {[Dy$_4$(HL)$_2$(L)$_4$(μ_3-OH)$_2$]·5MeOH·7H$_2$O} (**4**).* $Dy(NO_3)_3{\cdot}6H_2O$ (0.1 mmol) reacted with the Schiff-base H_2L formed by in situ condensation of ETA (0.3 mmol) and 3-formylsalicylic acid (0.3 mmol) in 10 mL of methanol. The yellow reaction solution was stirred for 3 h at room temperature and subsequently filtered. The filtrate was left undisturbed to allow slow evaporation of the solvent. After 2 days, when the reaction volume was around 2 mL, $Dy(NO_3)_3{\cdot}6H_2O$ (0.05 mmol) and Et_3N (0.1 mmol) were added to the reaction solution and subsequently closed by parafilm. Yellow single crystals of **4** suitable for X-ray diffraction analysis formed after 2 days. Yield: 29 mg (single crystals; 9% based on the metal salt). Anal. Calcd for $C_{65}H_{78}Dy_4N_6O_{31}$ (corresponds to **4**·$7H_2O$): C, 37.37; H, 3.76; N, 4.02%. Found: C, 37.82; H, 3.98; N, 4.45%. IR (ATR): ν 3060 (w, $\upsilon_{C=C-H}$), 2921 (br, υ_{C-H}), 2852 (w), 1641 (m), 1601 (m), 1551 (m), 1478 (w), 1456 (w), 1431 (w), 1363 (s), 1305 (w), 1272 (w), 1217 (m), 1150 (w), 1077 (w), 1048 (m), 967 (w), 872 (m), 830 (w), 757 (w), 645 (m), 627 (w), 573 (w), 553 (w) cm^{-1}.

*Synthesis of {[Dy$_4$(HL)$_8$(L)$_2$]·4MeOH·2H$_2$O} (**5**).* The Schiff-base H_2L was formed by in situ condensation of ETA (0.4 mmol) and 3-formylsalicylic acid (0.4 mmol) in 10 mL of methanol. $Dy(NO_3)_3{\cdot}6H_2O$ (0.13 mmol) and Et_3N (0.05 mmol) were added, and the reaction mixture was heated for 2 h at 80 °C. Then, the resulting yellow solution was filtered. The filtrate was left undisturbed to allow slow evaporation of the solvent. Yellow single crystals of **5** suitable for X-ray diffraction analysis formed within 1 week. Yield: 32 mg (single crystals; 8% based on the metal salt). Anal. Calcd for $C_{100}H_{106}Dy_4N_{10}O_{44}$ (corresponds to **5**·4MeOH): C, 42.87; H, 3.81; N, 5.00%. Found: C, 41.07; H, 3.99; N, 4.93%. IR (ATR): ν 3326 (br, υ_{OH}), 1646 (m), 1602 (m), 1543 (m), 1481 (w), 1456 (w), 1430 (w), 1373 (s), 1305 (w), 1269 (w), 1232 (w), 1212 (m), 1151 (w), 1080 (w), 1049 (m), 970 (w), 912 (w), 872 (m), 829 (w), 764 (m), 706 (w), 645 (w), 623 (w), 573 (w), 553 (w), 509 (w) cm^{-1}.

dx.doi.org/10.1021/ic5014957 | Inorg. Chem. 2015, 54, 773−781

Table 1. Crystallographic Details of 1−5

	1	2	3	4	5
chemical formula	$C_{42}H_{50}Y_1N_5O_{18}$	$C_{45}H_{62}Dy_1N_5O_{21}$	$C_{64}H_{82}N_6O_{34}Y_4$	$C_{65}H_{92}Dy_4N_6O_{38}$	$C_{104}H_{118}Dy_4N_{10}O_{46}$
fw g mol^{-1}	1001.78	1171.49	1834.99	2215.45	2894.08
cryst syst	monoclinic	monoclinic	monoclinic	monoclinic	monoclinic
a/Å	23.955(5)	14.035(3)	12.2239(5)	12.262(3)	14.6078(4)
b/Å	14.600(3)	25.654(4)	16.5807(5)	16.562(3)	15.2410(6)
c/Å	16.930(3)	17.380(3)	18.8528(8)	18.889(4)	25.4038(8)
β/deg	134.97(3)	123.94(2)	92.471(3)	92.60(3)	94.884(2)
unit cell volume/Å^3	4189(2)	5192.0(3)	3817.5(3)	3832.1(14)	5635.3(3)
temp/K	150	150(2)	150(2)	150(2)	100(2)
space group	$C2/c$	$P2_1/c$	$P2_1/c$	$P2_1/c$	$P2_1/n$
no. of formula units per unit cell, Z	4	4	2	2	2
radiation type	Mo Kα	Mo Kα	Mo Kα	Mo Kα	Mo Kα
μ/mm^{-1}	1.480	1.521	3.102	3.954	2.717
no. of reflns measd	11960	18971	29236	26541	26018
no. of indep reflns	3886	9652	7110	7527	10994
R_{int}	0.0818	0.0486	0.0813	0.0375	0.0989
final R1 values [$I > 2\sigma(I)$]	0.0549	0.0728	0.0558	0.0296	0.0591
final wR2(F^2) values (all data)	0.1337	0.1929	0.1467	0.0719	0.1598
GOF on F^2	0.885	1.128	1.032	1.065	0.947

Scheme 2. Synthesis of 1−5

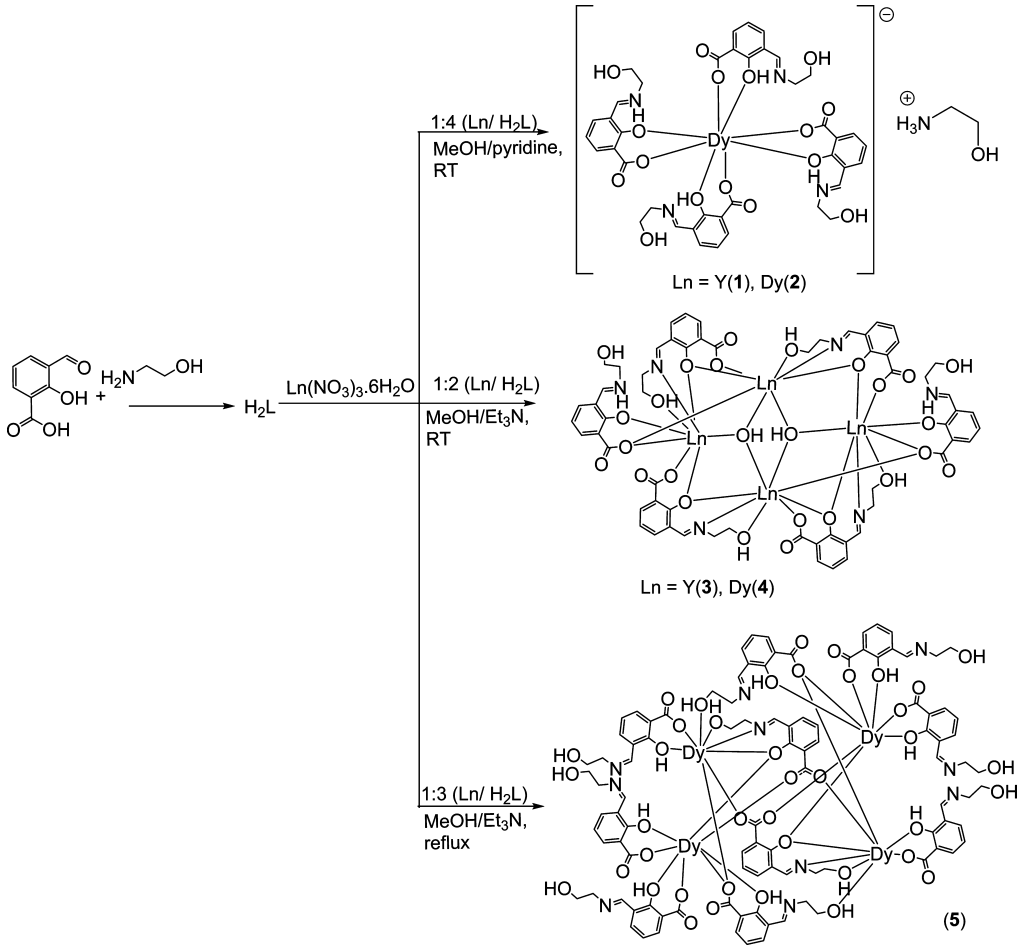

X-ray Crystallographic Studies of 1−5. A suitable crystal was covered in mineral oil (Aldrich) and mounted on a glass fiber. The crystal was transferred directly to a −73 or −123 °C cold stream of a STOE IPDS II diffractometer.

All structures were solved using the program *SHELXS-97*.[49] The remaining non-hydrogen atoms were located from successive Fourier difference map calculations. The refinements were carried out by using full-matrix least-squares techniques on F^2, minimizing the function $(F_o - F_c)^2$, where the weight is defined as $4F_o^2/2(F_o^2)$ and F_o and F_c are the observed and calculated structure factor amplitudes using the program *SHELXL-2013*.[49] The hydrogen atoms were placed in their calculated positions without refinement. The final values of the

dx.doi.org/10.1021/ic5014957 | *Inorg. Chem.* 2015, 54, 773−781

refinement parameters are given in Table 1. The locations of the largest peaks in the final difference Fourier map calculation as well as the magnitude of the residual electron densities in each case were of no chemical significance. The positional and thermal parameters and bond distances and angles have been deposited as Supporting Information (SI).

RESULTS AND DISCUSSION

Synthesis and Structures. The proligand Schiff-base H_2L was described before.[47] We prepared this ligand and characterized it again. During our investigation, we realized that an in situ preparation from 3-formylsalicylic and ETA without isolation of H_2L is most efficient. Thus, 3-formylsalicylic acid was allowed to react with ETA in different ratios and different reaction conditions in the presence of the metal salts $[Ln(NO_3)_3{\cdot}(H_2O)_6]$ (Ln = Y, Dy). By using pyridine as the base in methanol and a 1:4 Ln/H_2L ratio, the mononuclear complexes **1** and **2** were obtained at room temperature (Scheme 2). By using triethylamine as the base and a 1:2 (Ln/H_2L) ratio under similar reaction conditions, the planar tetranuclear clusters with butterfly structures **3** and **4** were isolated (Scheme 2). Upon a change in the metal-to-ligand ratio to 1:3 Ln/H_2L and an increase in the reaction temperature to 80 °C, the tetranuclear cluster **5**, which has a planar rectangular arrangement, was obtained (Scheme 2). All compounds could be isolated as single-crystalline materials directly from the reaction mixture. Obviously, the stoichiometric ratio and reaction conditions play a key role in the formation of different types of compounds. Compounds **1**−**5** were characterized by spectroscopic and analytical techniques. All complexes are poorly soluble in common organic solvents, and it was not possible to acquire NMR data. The solid-state structures were established by single-crystal X-ray diffraction.

Although the yttrium complex **1** crystallized in the monoclinic space group $C2/c$ and complex **2** crystallized in the monoclinic space group $P2_1/c$, the structures of the ionic complexes **1** and **2** are similar, differing only in the number of solvent molecules (MeOH and H_2O). Compounds **1** and **2** consist of a $[Ln(HL)_4]^-$ coordination anion and a protonated disordered ethanolamine $(ETAH)^+$ cation as well as disordered H_2O (**1**) or CH_3OH and H_2O molecules (**2**) (Figure1). In compound **1**, a crystallographic C_2 axis through the yttrium atom is observed, whereas in **2**, this symmetry axis is not observed and only a noncrystallographic pseudo-C_2 axis through the dysprosium atom is seen in the anion. However, the structural parameters of both compounds are similar. As a result of the asymmetric nature of the ligand, compounds **1** and **2** have a lower local symmetry on the metal than other recently published SIMs, e.g., $[Dy(AlMe_4)_3]$[22] and $(Bu_4N)[Tb(Pc)_2]$ (H_2Pc = phthalocyanine).[12] The structures of the anions are supported by ESI-MS data. The $[Ln(HL)_4]^-$ anion consists of one lanthanide(III) ion coordinated by four monoanionic Schiff-base ligands. Thus, the metal atom is eight-coordinated with four phenol oxygen atoms and four carboxyl oxygen atoms from the ligands, resulting in a distorted square-antiprismatic coordination polyhedron. Although some electron density is located between the phenol oxygen atom and the Schiff-base nitrogen atom (see Scheme 2), it is not possible to unambiguously assign the position of the remaining acidic proton of the ligand. However, on the basis of the pK_a values, we consider the benzoate function as deprotonated and the phenol as protonated in the ligand. The Ln−O (phenolate) and Ln−O (carboxyl) distances are in the ranges of 2.261(3)−2.264(3) Å (**1**) and 2.261(6)−2.330(6) Å (**2**) and 2.391(3)−2.392(3) Å (**1**) and 2.371(6)−2.383(6) Å (**2**), respectively. There is a very slight difference in the Ln−O bond lengths of the phenolic and carboxylic groups. Hydrogen bonds are observed between the proton of the alcohol function and the noncoordinating oxygen atom of the benzoate group. These bonds cause a folding of the ligand to give a compact structure without dangling arms.

Complexes **3** and **4** are isostructural and crystallize in the monoclinic space group $P2_1/c$, with half of the cluster and some disordered CH_3OH and H_2O molecules in the asymmetric unit (Figure 2). Only the number of solvent molecules (MeOH and H_2O), which could be refined, differ. Thus, we only describe here the structure of compound **4** in detail.

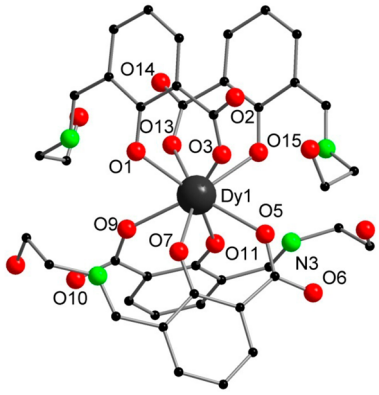

Figure 1. Solid-state structure of the anion of **2**. Shown is the coordination arrangement of a dysprosium atom, while omitting hydrogen atoms and solvent molecules for clarity. Color codes of the balls: Dy, dark gray; O, red; N, green; C, black.

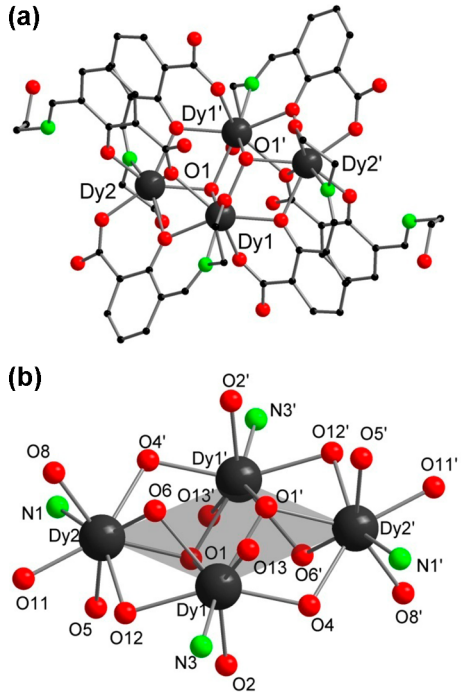

Figure 2. Solid-state structure of **4** (a) and side view of the planar Dy_4 core (b). All hydrogen atoms and solvent molecules have been omitted for clarity.

dx.doi.org/10.1021/ic5014957 | Inorg. Chem. 2015, 54, 773−781

A crystallographic inversion center is observed in the center of **4**. The dysprosium atoms are arranged with a planar rhomboidal scaffold. Such planar Dy_4 complexes are relatively rare.[43,44,50−52] The metal core of **4** consists of four dysprosium(III) ions (Dy1, Dy2, Dy1′, and Dy2′). In the center of the complex, two μ_3-hydroxide ligands bridge the central Dy1 and Dy1′ ions and one of the outer ions (Dy2 or Dy2′). These two μ_3-OH groups are nearly symmetrically arranged between the metal centers. The oxygen atoms (O1 and O1′) are located 0.923 Å out of the plane of the metal cores. The Dy2−O1 and Dy1−O1 distances are 2.327(3) and 2.356(3) Å and the Dy1′−O1−Dy1 and Dy2−O1−Dy1 angles are 108.00(12)° and 109.97(12)°, respectively. The periphery of the complex is bridged by the six Schiff-base ligands. Four ligands bind in a tetradentate μ_2-coordination mode with one carboxyl oxygen atom, the phenolate and alcohol oxygen atoms, and the Schiff-base nitrogen atom. We consider these four ligands as deprotonated at the phenol and at the acid function. The carboxyl and phenolate oxygen atoms of these ligands bind to one dysprosium atom, whereas the phenolate and alcohol oxygen atoms as well as the Schiff-base nitrogen atom bind to the adjacent dysprosium atom. The phenolate oxygen atoms of the four Schiff-base ligands adopt a μ_2-bridging mode. The remaining two Schiff-base ligands coordinate as observed in compound **2** in a κ^2-mode with the phenol and carboxyl oxygen atoms to the metal center. These two ligands are only singly negatively charged. The ligands adopt a μ_2-bridging mode in which the carboxylate oxygen atoms coordinate to Dy1 and Dy2. As was already reported for **1** and **2**, we can observe some electron density between the phenol oxygen atom and the Schiff-base nitrogen atom of these ligands (see Scheme 2), but we cannot unambiguously assign the position of the remaining acidic proton. All dysprosium ions are eight-coordinated from seven oxygen atoms and one imine nitrogen atom. A comparable coordination of the dysprosium atoms is observed, e.g., in $Dy_4(\mu_3\text{-}OH)_2(bmh)_2(msh)_4Cl_2]$ (H_2bmh = 1,2-bis(2-hydroxy-3-methoxybenzylidene)hydrazine; Hmsh = 3-methoxysalicylaldehyde hydrazone)[43] and $[Ln_4(\mu_3\text{-}OH)_2L'(acac)_6]\cdot 2CH_3CN$ (H_2L' = *N*,*N*′-bis(salicylidene)-*o*-phenylenediamine; acac = acetylacetonate).[44] All dysprosium atoms adopt a distorted square-antiprismatic geometry. The two square bases of the square antiprism for Dy1 consist of O1, O1′, O2, O4 and O6, O12, O13, N3, whereas for Dy2, the two square bases are defined by the atoms O1, O4, O5, N1 and O6, O8, O11, O12. Significant intramolecular hydrogen-bonding interaction has been observed between hydroxyl, carboxylic, and imine parts of the complex in the range 2.588−2.627 Å, and intermolecular hydrogen bonding was observed because of the presence of methanol and water molecules in the lattice, which are in the range 2.680−2.947 Å.

The tetranuclear complex **5** crystallizes in the monoclinic space group $P2_1/n$ with half of the molecule and some disordered CH_3OH and H_2O molecules in the asymmetric unit (Figure 3). A crystallographic inversion center is observed in the center of **5**. The four dysprosium ions, which are coordinated by 10 Schiff-base ligands, are arranged in a planar rectangular scaffold. The molecular structure consists of two binuclear subunits, in which each unit has two different types of dysprosium ions and four molecules of the ligand acting as a bridge to connect these subunits. Out of the 10 ligands that are coordinated to the metal atoms, two are double-deprotonated, whereas eight are only singly negatively charged. In contrast to **3** and **4**, the double-deprotonated ligands ($[L]^{2-}$) bind in a pentadentate mode to the metals. They are localized in the center of the cluster and bridge three dysprosium atoms each. The bridges are formed by the carboxylate and phenolate groups. Two singly negatively charged ligands ($[HL]^-$) bind, as it was observed in compound **2**, in a κ^2-mode with the phenol and carboxyl oxygen atoms in a chelating fashion to Dy1 and Dy1′. A third equiv of $[HL]^-$ binds in the same chelating mode to Dy1 or Dy1′ but also coordinates in a metal bridging mode via the carboxylate group to Dy2 or Dy2′. Furthermore, the alcohol function coordinates to a third dysprosium atom.

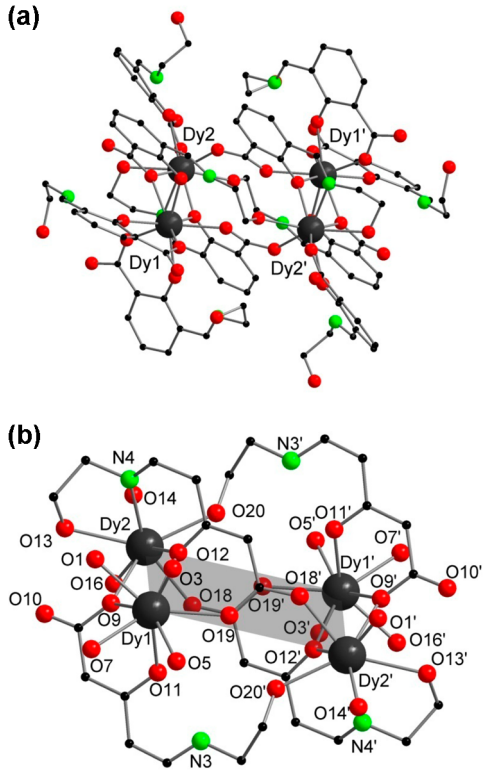

Figure 3. Solid-state structure of **5** (a) and side view of the planar rhombus Dy_4 core (b). All hydrogen atoms and solvent molecules have been omitted for clarity.

All dysprosium ions are eight-coordinated with different oxygen and nitrogen atoms of the Schiff-base ligands. Each dysprosium ion has a distorted square-antiprismatic geometry formed by eight oxygen atoms for Dy1 and seven oxygen atoms and one nitrogen atom for Dy2. The two square bases of the square antiprism for Dy1 consist of O1, O3, O5, O7 and O9, O11, O12, O19, whereas for Dy2, the two square bases are defined by the atoms O14, O16, O18, O20 and N4, O12, O9, O13. Dy1 and Dy2 are μ_2-bridging mode with the phenol and carboxylic oxygen atoms of the Schiff base with a Dy1−Dy2 distance of 3.8954(5) Å.

PL Properties. Ligand H_2L shows bright-greenish emission in the solid state. The intensity depends only moderately on the temperature within the range of 20−290 K. The emission is fluorescence with a lifetime shorter than 5 ns, as estimated using a nanosecond-pulsed nitrogen laser for excitation at 337 nm. The fluorescence spectrum of H_2L is centered at ∼490 nm at 290 K but shifts to 540 nm at 20 K (Figure 4). The PLQY was determined to be 0.20 (20%) at ambient temperature. This relatively high value may even be slightly underestimated because of the overlap (relatively small Stokes shift) between the PL excitation (absorption) and emission spectra, resulting

dx.doi.org/10.1021/ic5014957 | *Inorg. Chem.* 2015, 54, 773−781

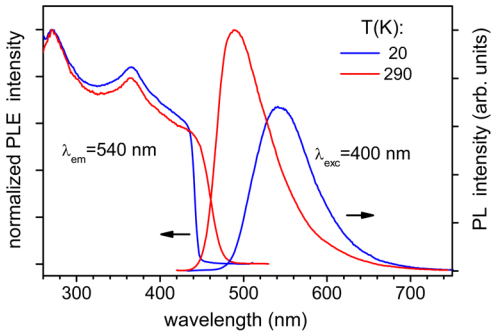

Figure 4. PL excitation (PLE) and emission (PL) spectra (left and right panels, respectively) of solid compound H_2L at temperatures of 20 and 290 K. The PL and PLE spectra were excited and recorded at 400 and 540 nm, respectively.

in reabsorption of the shorter-wavelength emission in the bulk (crystalline powder) sample of H_2L. Note that the same remark is also true for complexes **1** and **4** and, in particular, for complex **3**, whose PL properties have been studied in this work (Figures 5−7).

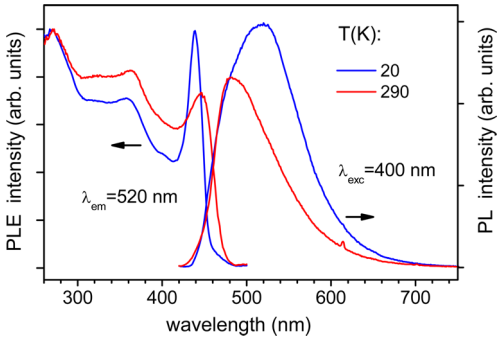

Figure 5. PLE and PL spectra of solid compound **1** at 20 and 290 K.

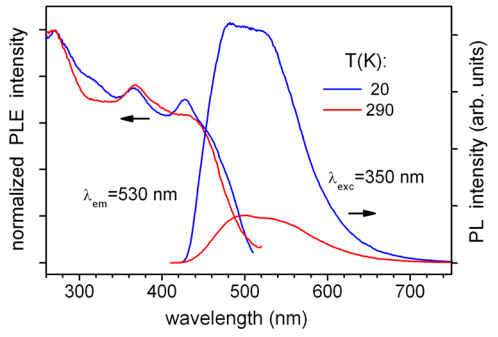

Figure 6. PLE and PL spectra (left and right panels, respectively) of solid compound **3** at temperatures of 20 and 290 K. The PL and PLE spectra were excited and recorded at 400 and 540 nm, respectively.

PLE and PL spectra of the above complexes, as well as their emission lifetimes (<5 ns), are roughly similar to those of H_2L (cf. Figures 4−7). There are also similar (less pronounced) red shifts of the PL maximum and PLE absorption onset, which are observed on decreasing temperature. Therefore, we conclude that the visible PL of complexes **1**, **3**, and **4** is ligand-based, with a moderate influence through ligand−metal and ligand−ligand interactions in the solid state. Similar to H_2L, the greenish emission of Y and Y_4 complexes **1** and **3** is rather strong. The corresponding PLQY values amount to 11.5 and 13%,

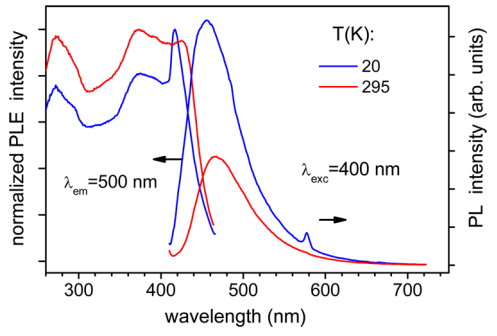

Figure 7. PLE and PL spectra of solid complex **4** at temperatures of 20 and 295 K. The PL and PLE spectra were excited and recorded at 300 and 500 nm, respectively. A "shoulder" on the emission curve (T = 20 K) at ∼485 nm and a peak at 577 nm are due to f−f emission lines of dysprosium(III).

respectively, at ambient temperature. The PL intensity increases by decreasing temperature, e.g., on a factor of ∼4 for complex **3** below ∼100 K (Figure 6). As a result, a PLQY of about 60% is expected for this complex at lowest temperatures. Different from the case for H_2L and the Dy_4 complex **4**, the emission band of **1** and particularly of **3** is broadened and asymmetrically shaped at both ambient and low temperatures (Figures 5 and 6). This likely indicates a contribution of several excited ligand substates/configurations, emitting at slightly different energies. A distorted, "hat-like" shape of the emission band of **3** can also be explained, in part, by the strong overlap (small Stokes shift) of the PLE and PL spectra of this complex and emission reabsorption effects.

In contrast to **1** and **3**, the dysprosium complex **4** shows relatively weak ligand-based fluorescence centered at ∼455 and 465 nm at 20 and 295 K, respectively (Figure 7). Its PLQY was determined to be only 0.7% at T = 295 K, which is probably due to a quenching effect of the dysprosium ions. There is some energy transfer to excited electronic levels of dysprosium, as evidenced by the characteristic f−f emission lines of dysprosium(III) in the visible spectral range at ∼485 and 577 nm (observed at low temperatures), as well as in the near-IR region, e.g., at 845, 940, 1015, and 1184 nm (Figure S1 in the SI). These lines can be assigned to the $^4F_{9/2} \rightarrow {}^6H_J$, $J = {}^{15}/_2$, ${}^{13}/_2$, and ${}^5/_2$, and $^4F_{9/2} \rightarrow {}^6F_J$, $J = {}^7/_2$, ${}^5/_2$, and ${}^3/_2$ transitions, respectively. However, the energy-transfer efficiency is apparently low because the dysprosium(III) emission is weak. The latter appears to be sensitized only via the ligand singlet state [cf. the ligand-based fluorescence at ∼455 nm with regard to the resonant $^4F_{9/2}$ state of dysprosium(III) at ∼485 nm]. The generally more efficient triplet-to-lanthanide energy transfer is not expected in **4** because the ligand triplet state, even if generated significantly, likely lies below the $^4F_{9/2}$ state. Interestingly, although the integrated emission intensity of dysprosium(III) in **4** increases only moderately on decreasing temperature, the relative intensities of particular f−f transitions vary strongly. For instance, a peak at ∼845 nm assigned to the $^4F_{9/2} \rightarrow {}^6H_{5/2}$ transition is quite prominent at 20 K but nearly missing at 290 K (Figure S2 in the SI).

Magnetic Properties of Compounds 2, 4, and 5. The static dc magnetic susceptibility studies of **2** were performed in the 1.8−300 K range under an applied magnetic field of 1000 Oe (Figure 8). The χT value of 15.0 cm^3 K mol^{-1} at 300 K for **2** is close to the calculated value of 14.17 cm^3 K mol^{-1} for the ground state of the dysprosium(III) ion ($4f^9$, $J = {}^{15}/_2$, $S = {}^5/_2$, L

dx.doi.org/10.1021/ic5014957 | Inorg. Chem. 2015, 54, 773−781

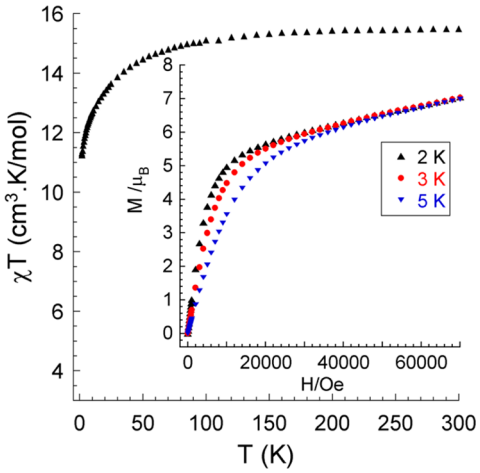

Figure 8. Temperature dependence of χT for compound **2** at 1000 Oe. Inset: molar magnetization versus field at 2−5 K.

= 5, g = $^4/_3$, and $^6H_{15/2}$). Upon cooling, the χT product gradually decreases to achieve a value of 11.1 cm^3 K mol^{-1} at 1.8 K. Such behavior is primarily due to the depopulation of the Stark sublevels of the dysprosium ion, which occurs from the splitting of the $^6H_{15/2}$ ground term by the ligand field. The M versus H plot at 2−5 K (inset in Figure 8) shows a quite fast increase in magnetization at low field (until 1 T) and then a slow linear increase to achieve a value of 7.0 μ_B at the maximum applied field of 7 T. This value is lower than the expected saturation value for dysprosium(III) of ∼10 μ_B, and such a behavior is likely due to crystal-field effects leading to significant magnetic anisotropy. Dynamic alternating-current (ac) magnetic susceptibility measurements as a function of the temperature were carried out, but this complex did not show any out-of-phase signal under zero or dc external field.

The dc magnetic data for complex **4** shows temperature-dependent values of χT of 56.1−59.0 cm^3 K mol^{-1} over the temperature range 300−50 K (Figure 9). On decreasing the

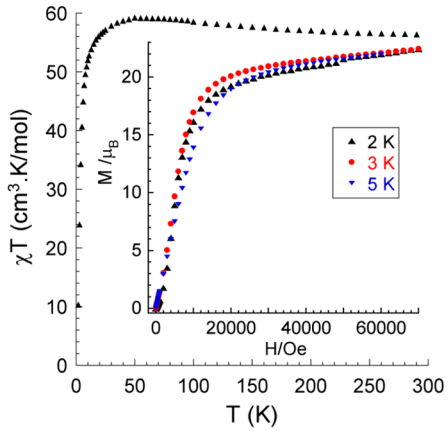

Figure 9. Temperature dependence of χT for compound **4** at 1000 Oe. Inset: molar magnetization versus field at 2−5 K.

temperature, χT drops abruptly to a minimum value of 10 cm^3 K mol^{-1} at 2 K, indicating depopulation of excited Stark sublevels. Magnetization data at low temperatures are shown in the inset of Figure 9. The magnetization at all temperatures (2−5 K) reaches a maximum value of 22.8 μ_B at 70000 Oe, without showing true saturation. This is noticeably lower than the theoretical value for four dysprosium(III) ions (∼40 μ_B), indicating a much smaller effective spin in **4**. Isothermal magnetization experiments done at 2.0 K show hysteresis with a small coercive field of 9 Oe and a small remanent magnetization of 0.012 μ_B (Figure S3 in the SI). From the magnetization curve at 2 K, two inflections (one at ∼1500 Oe and a second at ∼40000 Oe) are observed. Such types of inflections are usually observed when the applied magnetic fields overcome intra- and/or intermolecular antiferromagnetic interactions and alignment of the spins occurs. Because the spin ground state in a dysprosium(III)-containing compound is difficult to characterize, it is also difficult to conclude about the degree of magnetic interactions and processes responsible for the features observed at those two regions.

The relaxation of magnetization for a polycrystalline sample **4** was studied using temperature- and frequency-dependent ac susceptibility measurements (Figures S4 in the SI and 10). The ac data measured at zero applied field for frequencies between 1 and 1500 Hz show frequency dependence of the out-of-phase signals belonging to two relaxation processes (Figure S4 in the SI).

The data in the χ'' versus frequency plot (Figure 10) were extracted to give an Arrhenius plot (ln τ vs $1/T$; Figure S5 in the SI), and linear fitting of the high-temperature region (slow relaxation, SR) resulted in a relaxation time of $\tau_0 = 5.1 \times 10^{-9}$ s and a barrier of U_{eff} = 84 K, pertaining to the relaxation mechanism assigned to a thermally activated process. Figure S4 in the SI also shows a second relaxation mechanism that is essentially below 6 K (fast relaxation, FR), with $\tau_0 = 2.5 \times 10^{-3}$ s and a barrier of U_{eff} = 3 K. Arrhenius analysis confirms that both processes are thermally activated, but the τ_0 value obtained for the FR is much larger than expected for a SMM[15,53,54] and, in contrast to other reported Dy_4 compounds,[30,55,56] strongly suggests that this process is dominated by quantum effects. An alternative reason for the appearance of low-temperature relaxation might be due to weak dipolar or intermolecular interactions through hydrogen bonds.

The dc magnetic data (Figure S6 in the SI) for complex **5** show only small differences compared with compound **4**. However, it shows no frequency dependence of the ac susceptibility in zero and nonzero applied field.

SUMMARY

Five new rare-earth compounds that are ligated by HL$^-$ and in some cases also with the corresponding dianion L^{2-} were prepared. Depending on the stoichiometric ratio, either mononuclear or tetranuclear complexes were obtained. The clusters are either in a butterfly or in a rectangular scaffold arrangement. The proligand H_2L and all yttrium complexes show bright-greenish fluorescence in the solid state at ambient temperature with quantum yields of up to 20%. In contrast, the dysprosium compound **4** shows weak ligand fluorescence and very weak dysprosium(III) emission lines likely due to quenching effects. In the magnetic studies, the tetranuclear compound **4** with the butterfly structure shows SMM behavior with two relaxation processes. In comparison to the tetranuclear compound **4**, the mononuclear compound **2** and the tetranuclear compound **5** with rectangular arrangement show no slow relaxation of magnetization.

dx.doi.org/10.1021/ic5014957 | Inorg. Chem. 2015, 54, 773−781

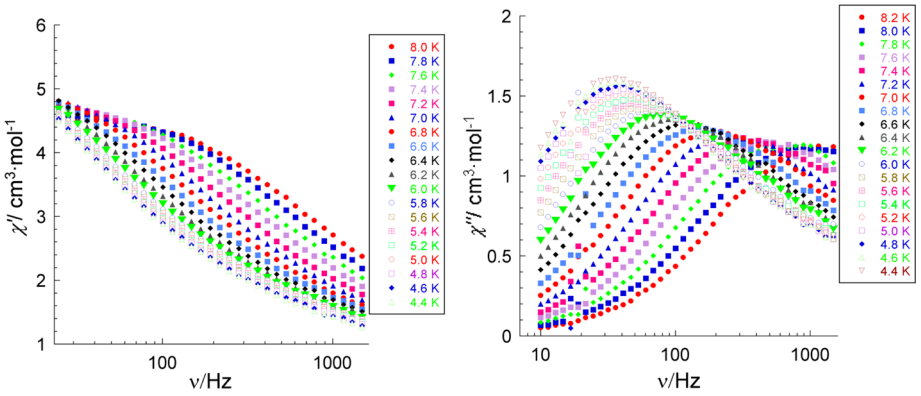

Figure 10. In-phase (χ') and out-of-phase (χ'') ac susceptibility versus frequency ν on a logarithmic scale for **4** over the temperature range 4.4−8.0 K.

■ ASSOCIATED CONTENT

Ⓢ Supporting Information

X-ray crystallographic files in CIF format for the structure determination of **1**−**5** and additional information about the PL and magnetic measurements. This material is available free of charge via the Internet at http://pubs.acs.org.

■ AUTHOR INFORMATION

Corresponding Authors

*E-mail: Manfred.Kappes@kit.edu.
*E-mail: annie.powell@kit.edu.
*E-mail: roesky@kit.edu.

Notes

The authors declare no competing financial interest.

■ ACKNOWLEDGMENTS

This work was supported by the DFG Center for Functional Nanostructures and the DFG-funded transregional collaborative research center SFB/TRR 88 "3MET".

■ DEDICATION

Dedicated to the memory of Prof. John Corbett.

■ REFERENCES

(1) Bogani, L.; Wernsdorfer, W. *Nat. Mater.* **2008**, *7*, 179−186.
(2) Leuenberger, M. N.; Loss, D. *Nature* **2001**, *410*, 789−793.
(3) Yamanouchi, M.; Chiba, D.; Matsukura, F.; Ohno, H. *Nature* **2004**, *428*, 539−542.
(4) Saitoh, E.; Miyajima, H.; Yamaoka, T.; Tatara, G. *Nature* **2004**, *432*, 203−206.
(5) Gatteschi, D.; Caneschi, A.; Pardi, L.; Sessoli, R. *Science* **1994**, *265*, 1054−1058.
(6) Bagai, R.; Christou, G. *Chem. Soc. Rev.* **2009**, *38*, 1011−1026.
(7) Rinehart, J. D.; Fang, M.; Evans, W. J.; Long, J. R. *Nat. Chem.* **2011**, *3*, 538−542.
(8) Blagg, R. J.; Ungur, L.; Tuna, F.; Speak, J.; Comar, P.; Collison, D.; Wernsdorfer, W.; McInnes, E. J. L.; Chibotaru, L. F.; Winpenny, R. E. P. *Nat. Chem.* **2013**, *5*, 673−678.
(9) Rinehart, J. D.; Long, J. R. *Chem. Sci.* **2011**, *2*, 2078−2085.
(10) Yamashita, A.; Watanabe, A.; Akine, S.; Nabeshima, T.; Nakano, M.; Yamamura, T.; Kajiwara, T. *Angew. Chem., Int. Ed.* **2011**, *50*, 4016−4019.
(11) Kajiwara, T.; Nakano, M.; Takahashi, K.; Takaishi, S.; Yamashita, M. *Chem.—Eur. J.* **2011**, *17*, 196−205.
(12) Ishikawa, N.; Sugita, M.; Ishikawa, T.; Koshihara, S.-y.; Kaizu, Y. *J. Am. Chem. Soc.* **2003**, *125*, 8694−8695.
(13) Ishikawa, N.; Sugita, M.; Ishikawa, T.; Koshihara, S.-y.; Kaizu, Y. *J. Chem. Phys. B* **2004**, *108*, 11265−11271.
(14) Jiang, S.-D.; Wang, B.-W.; Su, G.; Wang, Z.-M.; Gao, S. *Angew. Chem., Int. Ed.* **2010**, *49*, 7448−7451.
(15) Cucinotta, G.; Perfetti, M.; Luzon, J.; Etienne, M.; Car, P.-E.; Caneschi, A.; Calvez, G.; Bernot, K.; Sessoli, R. *Angew. Chem., Int. Ed.* **2012**, *51*, 1606−1610.
(16) Zhang, P.; Guo, Y.-N.; Tang, J. *Coord. Chem. Rev.* **2013**, *257*, 1728−1763.
(17) Luzon, J.; Sessoli, R. *Dalton Trans.* **2012**, *41*, 13556−13567.
(18) Anwar, M. U.; Thompson, L. K.; Dawe, L. N.; Habib, F.; Murugesu, M. *Chem. Commun.* **2012**, *48*, 4576−4578.
(19) Sorace, L.; Benelli, C.; Gatteschi, D. *Chem. Soc. Rev.* **2011**, *40*, 3092−3104.
(20) Sessoli, R.; Powell, A. K. *Coord. Chem. Rev.* **2009**, *253*, 2328−2341.
(21) Demir, S.; Zadrozny, J. M.; Nippe, M.; Long, J. R. *J. Am. Chem. Soc.* **2012**, *134*, 18546−18549.
(22) König, S. N.; Chilton, N. F.; Maichle-Mössmer, C.; Pineda, E. M.; Pugh, T.; Anwander, R.; Layfield, R. A. *Dalton Trans.* **2014**, *43*, 3035−3038.
(23) Das, S.; Hossain, S.; Dey, A.; Biswas, S.; Sutter, J.-P.; Chandrasekhar, V. *Inorg. Chem.* **2014**, *53*, 5020−5028.
(24) Thielemann, D. T.; Wagner, A. T.; Lan, Y.; Anson, C. E.; Gamer, M. T.; Powell, A. K.; Roesky, P. W. *Dalton Trans.* **2013**, *42*, 14794−14800.
(25) Gao, F.; Cui, L.; Liu, W.; Hu, L.; Zhong, Y.-W.; Li, Y.-Z.; Zuo, J.-L. *Inorg. Chem.* **2013**, *52*, 11164−11172.
(26) Fatila, E. M.; Rouzières, M.; Jennings, M. C.; Lough, A. J.; Clérac, R.; Preuss, K. E. *J. Am. Chem. Soc.* **2013**, *135*, 9596−9599.
(27) Ungur, L.; Thewissen, M.; Costes, J.-P.; Wernsdorfer, W.; Chibotaru, L. F. *Inorg. Chem.* **2013**, *52*, 6328−6337.
(28) Anwar, M. U.; Dawe, L. N.; Tandon, S. S.; Bunge, S. D.; Thompson, L. K. *Dalton Trans.* **2013**, *42*, 7781−7794.
(29) Chandrasekhar, V.; Dey, A.; Das, S.; Rouzières, M.; Clérac, R. *Inorg. Chem.* **2013**, *52*, 2588−2598.
(30) Chandrasekhar, V.; Hossain, S.; Das, S.; Biswas, S.; Sutter, J.-P. *Inorg. Chem.* **2013**, *52*, 6346−6353.
(31) Suzuki, K.; Sato, R.; Mizuno, N. *Chem. Sci.* **2013**, *4*, 596−600.
(32) Le Roy, J. J.; Jeletic, M.; Gorelsky, S. I.; Korobkov, I.; Ungur, L.; Chibotaru, L. F.; Murugesu, M. *J. Am. Chem. Soc.* **2013**, *135*, 3502−3510.
(33) Wang, Y.-X.; Shi, W.; Li, H.; Song, Y.; Fang, L.; Lan, Y.; Powell, A. K.; Wernsdorfer, W.; Ungur, L.; Chibotaru, L. F.; Shen, M.; Cheng, P. *Chem. Sci.* **2012**, *3*, 3366−3370.
(34) Tuna, F.; Smith, C. A.; Bodensteiner, M.; Ungur, L.; Chibotaru, L. F.; McInnes, E. J. L.; Winpenny, R. E. P.; Collison, D.; Layfield, R. A. *Angew. Chem., Int. Ed.* **2012**, *51*, 6976−6980.
(35) Anwar, M. U.; Thompson, L. K.; Dawe, L. N.; Habib, F.; Murugesu, M. *Chem. Commun.* **2012**, *48*, 4576−4578.

(36) Lin, S.-Y.; Wernsdorfer, W.; Ungur, L.; Powell, A. K.; Guo, Y.-N.; Tang, J.; Zhao, L.; Chibotaru, L. F.; Zhang, H.-J. *Angew. Chem., Int. Ed.* **2012**, *51*, 12767−12771.
(37) Blagg, R. J.; Muryn, C. A.; McInnes, E. J. L.; Tuna, F.; Winpenny, R. E. P. *Angew. Chem., Int. Ed.* **2011**, *50*, 6530−6533.
(38) Chen, G.-J.; Gao, C.-Y.; Tian, J.-L.; Tang, J.; Gu, W.; Liu, X.; Yan, S.-P.; Liao, D.-Z.; Cheng, P. *Dalton Trans.* **2011**, *40*, 5579−5583.
(39) Abbas, G.; Lan, Y.; Kostakis, G. E.; Wernsdorfer, W.; Anson, C. E.; Powell, A. K. *Inorg. Chem.* **2010**, *49*, 8067−8072.
(40) Habib, F.; Lin, P.-H.; Long, J.; Korobkov, I.; Wernsdorfer, W.; Murugesu, M. *J. Am. Chem. Soc.* **2011**, *133*, 8830−8833.
(41) AlDamen, M. A.; Cardona-Serra, S.; Clemente-Juan, J. M.; Coronado, E.; Gaita-Ariño, A.; Martí-Gastaldo, C.; Luis, F.; Montero, O. *Inorg. Chem.* **2009**, *48*, 3467−3479.
(42) Gamer, M. T.; Lan, Y.; Roesky, P. W.; Powell, A. K.; Clérac, R. *Inorg. Chem.* **2008**, *47*, 6581−6583.
(43) Lin, P.-H.; Burchell, T. J.; Ungur, L.; Chibotaru, L. F.; Wernsdorfer, W.; Murugesu, M. *Angew. Chem., Int. Ed.* **2009**, *48*, 9489−9492.
(44) Sun, W.-B.; Han, B.-L.; Lin, P.-H.; Li, H.-F.; Chen, P.; Tian, Y.-M.; Murugesu, M.; Yan, P.-F. *Dalton Trans.* **2013**, *42*, 13397−13403.
(45) Roesky, P. W.; Bhunia, A.; Lan, Y.; Powell, A. K.; Kureti, S. *Chem. Commun.* **2011**, *47*, 2035−2037.
(46) Bhunia, A.; Gamer, M. T.; Ungur, L.; Chibotaru, L. F.; Powell, A. K.; Lan, Y.; Roesky, P. W.; Menges, F.; Riehn, C.; Niedner-Schatteburg, G. *Inorg. Chem.* **2012**, *51*, 9589−9597.
(47) Maurya, M. R.; Kumar, U.; Manikandan, P. *Eur. J. Inorg. Chem.* **2007**, 2303−2314.
(48) Lebedkin, S.; Langetepe, T.; Sevillano, P.; Fenske, D.; Kappes, M. M. *J. Chem. Phys. B* **2002**, *106*, 9019−9026.
(49) Sheldrick, G. M. *Acta Crystallogr., Sect. A* **2008**, *64*, 112−122.
(50) Zheng, Y.-Z.; Lan, Y.; Anson, C. E.; Powell, A. K. *Inorg. Chem.* **2008**, *47*, 10813−10815.
(51) Yan, P.-F.; Lin, P.-H.; Habib, F.; Aharen, T.; Murugesu, M.; Deng, Z.-P.; Li, G.-M.; Sun, W.-B. *Inorg. Chem.* **2011**, *50*, 7059−7065.
(52) Langley, S. K.; Chilton, N. F.; Gass, I. A.; Moubaraki, B.; Murray, K. S. *Dalton Trans.* **2011**, *40*, 12656−12659.
(53) Jiang, S.-D.; Liu, S.-S.; Zhou, L.-N.; Wang, B.-W.; Wang, Z.-M.; Gao, S. *Inorg. Chem.* **2012**, *51*, 3079−3087.
(54) Meihaus, K. R.; Rinehart, J. D.; Long, J. R. *Inorg. Chem.* **2011**, *50*, 8484−8489.
(55) Chandrasekhar, V.; Das, S.; Dey, A.; Hossain, S.; Sutter, J.-P. *Inorg. Chem.* **2013**, *52*, 11956−11965.
(56) Xue, S.; Zhao, L.; Guo, Y.-N.; Chen, X.-H.; Tang, J. *Chem. Commun.* **2012**, *48*, 7031−7033.